

A diffusion generated method for computing Dirichlet partitions

Dong Wang, Braxton Osting*

Department of Mathematics, University of Utah, Salt Lake City, UT

Abstract

A Dirichlet k -partition of a closed d -dimensional surface is a collection of k pairwise disjoint open subsets such that the sum of their first Laplace-Beltrami-Dirichlet eigenvalues is minimal. In this paper, we develop a simple and efficient diffusion generated method to compute Dirichlet k -partitions for d -dimensional flat tori and spheres. For the $2d$ flat torus, for most values of $k = 3, 9, 11, 12, 15, 16$, and 20 , we obtain hexagonal honeycombs. For the $3d$ flat torus and $k = 2, 4, 8, 16$, we obtain the rhombic dodecahedral honeycomb, the Weaire-Phelan honeycomb, and Kelvin's tessellation by truncated octahedra. For the $4d$ flat torus, for $k = 4$, we obtain a constant extension of the rhombic dodecahedral honeycomb along the fourth direction and for $k = 8$, we obtain a 24-cell honeycomb. For the $2d$ sphere, we also compute Dirichlet partitions for $k = 3, 7, 9, 10, 12, 14, 20$. Our computational results agree with previous studies when a comparison is available. As far as we are aware, these are the first published results for Dirichlet partitions of the $4d$ flat torus.

Keywords: Dirichlet partition, diffusion generated method, honeycomb, Weaire-Phelan structure, Kelvin structure, 24-cell

2010 MSC: 49Q10, 35R01, 05B45

*B. Osting is partially supported by NSF DMS 16-19755.

*Corresponding author

Email addresses: dwang@math.utah.edu (Dong Wang), osting@math.utah.edu (Braxton Osting)

1. Introduction

For $d \geq 2$, let U be either an open bounded domain in \mathbb{R}^d with Lipschitz boundary or a closed, smooth, d -dimensional manifold. For $k \geq 2$ fixed, the *Dirichlet k -partition problem* for U is to choose a k -partition, *i.e.*, k disjoint quasi-open sets $U_1, U_2, \dots, U_k \subseteq U$, that attains

$$\min_{U = \bigcup_{\ell \in [k]} U_\ell} \sum_{\ell \in [k]} \lambda_1(U_\ell) \quad (1)$$

where

$$\lambda_1(U) := \min_{\substack{u \in H_0^1(U) \\ \|u\|_{L^2(U)} = 1}} E(u) \quad \text{and} \quad E(u) := \begin{cases} \int_U |\nabla u|^2 \, dx & u \in H_0^1(U) \\ \infty & \text{otherwise} \end{cases}. \quad (2)$$

Here, E is the Dirichlet energy and $\lambda_1(U)$ is the first Dirichlet eigenvalue of the Laplace-Beltrami operator, $-\Delta$, on U with Dirichlet boundary conditions imposed on ∂U . We refer to any k -partition that attains the minimum in (1) as a *Dirichlet k -partition of U* , or simply a *Dirichlet partition* when k and U are understood. Observe that by the monotonicity of Dirichlet eigenvalues, any Dirichlet partition satisfies $\overline{U} = \cup_{i=1}^k \overline{U_i}$, which justifies the use of the word “partition” in the name. The existence of optimal partitions in the class of quasi-open sets was proved in [1] and, subsequently, several papers have investigated properties of optimal partitions including the regularity of the partition interfaces and the asymptotic behavior as $k \rightarrow \infty$ [2, 3, 4]. Dirichlet partitions arise in the study of Bose-Einstein condensates [5, 6, 7], models for interacting agents [8, 9, 7, 10, 11], and have recently been studied in the context of data analysis [12, 13, 14].

1.1. Results

In this paper, we develop an efficient diffusion generated method for computing Dirichlet partitions of d -dimensional flat tori and spheres; see Algorithm 1. The method is best motivated by a mapping formulation of Dirichlet partitions that we review in Section 2. The method is very simple, consisting of iterating

the following three steps: (i) Evolve k functions on U by the diffusion equation until time τ . (ii) At each point of U , find which of the k functions is largest and set the other functions to zero. (iii) Renormalize each of the k functions. This method is implemented using the Fast Fourier Transform (FFT) and Spherical Harmonic Transform (SHT), as described in Section 3.

in Section 4, we present results of extensive numerical experiments. For the $2d$ flat torus, for most values of $k = 3, 9, 11, 12, 15, 16$, and 20 , we obtain hexagonal honeycombs. For the $3d$ flat torus and $k = 2, 4, 8, 16$, we obtain the rhombic dodecahedral honeycomb, the Weaire-Phelan honeycomb, and Kelvin's tessellation by truncated octahedra. For the $4d$ flat torus and $k = 4$, we obtain a constant extension of the rhombic dodecahedral honeycomb along the fourth direction and for $k = 8$, we obtain a 24-cell honeycomb. For the $2d$ sphere, we also compute Dirichlet partitions for $k = 3, 7, 9, 10, 12, 14, 20$. Our results agree with previous studies when a comparison is available. As far as we are aware, these are the first published results for Dirichlet partitions of the $4d$ flat torus.

For each of the flat tori considered, we have fixed a periodic box and the value k and approximate the optimal partition. This is an easier problem than determining the optimal partition as $k \rightarrow \infty$. It has been observed that, for two-dimensional domains, as $k \rightarrow \infty$, a regular tiling of hexagons is optimal [4]. In four dimensions, our computational study suggests that, as $k \rightarrow \infty$, a regular 24-cell honeycomb is a good candidate minimizer.

2. A diffusion generated method for computing Dirichlet partitions

In this section we first describe a mapping reformulation of the Dirichlet partitioning problem, (1). Motivated by the formulation of the problem, we introduce an efficient diffusion generated method for computing Dirichlet partitions; see Section 2.2. A brief comparison of our method with previous methods is given in Section 2.3

2.1. Mapping reformulation of Dirichlet partitions

Let Σ_k denote the coordinate axis in \mathbb{R}^k and define the Sobolev space

$$H_0^1(U; \Sigma_k) = \{\mathbf{u} \in H_0^1(U; \mathbb{R}^k) : \mathbf{u}(x) \in \Sigma_k \text{ a.e.}\}.$$

Since at most one component of a vector $\mathbf{v} \in \Sigma_k$ is non-zero, it follows that if $\mathbf{u} \in H_0^1(U; \Sigma_k)$ is continuous, then the sets $U_\ell = u_\ell^{-1}(\mathbb{R} \setminus \{0\})$ partition U .

The Dirichlet partition problem for U is equivalent to the mapping problem

$$\min \left\{ \mathbf{E}(\mathbf{u}) : \mathbf{u} = (u_1, \dots, u_k) \in H_0^1(U; \Sigma_k), \int_U u_\ell^2(x) dx = 1 \forall \ell \in [k] \right\}, \quad (3)$$

where $\mathbf{E}(\mathbf{u}) := \sum_{\ell=1}^k \int_U |\nabla u_\ell|^2 dx$ is the Dirichlet energy of \mathbf{u} [2]. We refer to a solution of (3) as a *ground state of U* , which, without loss of generality, we may assume to be nonnegative. In particular, if \mathbf{u} is a quasi-continuous representative of a ground state such that each component function u_ℓ assumes only nonnegative values, then a Dirichlet partition $U = \Pi_\ell U_\ell$ is given by $U_\ell = u_\ell^{-1}(0, \infty)$ for $\ell = 1, \dots, k$. Likewise, the first Dirichlet eigenvectors u_ℓ of a Dirichlet partition $\Pi_\ell U_\ell$ may be assembled into a function $\mathbf{u} \in H_0^1(U; \Sigma_k)$ that solves the mapping problem (3).

2.2. Computational methods for Dirichlet partitions

We consider the mapping formulation for Dirichlet partitions, (3), for which there are basically three ingredients: (i) the Dirichlet energy, (ii) the constraint that $u(x) \in \Sigma_k$, and (iii) the constraint that $\int_U u_\ell^2 = 1$. Algorithm 1 iteratively handling these three ingredients. We begin with an initial vector valued function $\mathbf{u}^0 \in H_0^1(U; \mathbb{R}^k)$. Since $\Sigma_k \subset \mathbb{R}^k$, we can consider the unconstrained gradient flow of the Dirichlet energy until time τ , which is exactly the evolution by the diffusion equation, given in the Diffusion Step of Algorithm 1. Let $\tilde{u}_\ell(x) = u_\ell(\tau, x)$ denote the solution at time $\tau > 0$. Next, for each point $x \in U$, we consider the closest value in Σ_k to $\tilde{u}(x)$. This is exactly the Projection Step of Algorithm 1. In this step, a rule should be devised to break any ties, but in practice we do not observe any. Finally, we renormalize each component

of the vector to satisfy the $L^2(U)$ constraint as in the Renormalization Step of Algorithm 1. These three steps are iterated until the condition that the partitions memberships didn't change in the previous iteration, i.e.,

$$\sum_{\ell \in [k]} \|\chi_{\{u_\ell^s > 0\}} - \chi_{\{u_\ell^{s-1} > 0\}}\| = 0 \quad (4)$$

where $\chi_{\{\cdot\}}$ denotes the indicator function.

We refer to this algorithm as “diffusion generated” as it contains a diffusion step, similar to the Merriman-Bence-Osher (MBO) diffusion generated motion for approximating mean curvature flow [15, 16, 17]. This method has subsequently been extensively analyzed and extended to more general contexts; see [18, 19, 20].

2.3. Comparison with other methods for computing Dirichlet partitions

There are variety of approaches to computing Dirichlet partitions, which we organize by the way in which the energy (1), or equivalently (3), is relaxed.

One relaxation of the constraint $\mathbf{u}(x) \in \Sigma_k$ is the following. Consider the function $f: \mathbb{R}^k \rightarrow \mathbb{R}$, given by $f(x) = \sum_{i \neq j}^k x_i^2 x_j^2$. It is not difficult to see that $f(x) \geq 0$ and $\Sigma_k = f^{-1}(0)$. For $\varepsilon > 0$, we can consider the relaxation of (3), given by

$$\min \left\{ \mathbf{E}^\varepsilon(\mathbf{u}): \mathbf{u} = (u_1, \dots, u_k) \in H_0^1(U; \mathbb{R}^k), \int_U u_\ell^2(x) dx = 1 \forall \ell \in [k] \right\}, \quad (5)$$

where the relaxed energy is given by $\mathbf{E}^\varepsilon(\mathbf{u}) := \mathbf{E}(\mathbf{u}) + \frac{1}{2\varepsilon^2} \int_U f(\mathbf{u}(x)) dx$. Properties of this relaxation can be found in [6, 2] and it was used to devise computational methods in [6, 21, 22].

In particular, in [21], Q. Du and F. Lin introduce a three-step diffusion generated motion similar to the one considered in Algorithm 1. However, in the second step, rather than taking the closest point in Σ_k , the following system of ODEs is solved until time τ ,

$$\frac{d}{dt} \tilde{u}_\ell = \frac{1}{\varepsilon^2} \left(\sum_{j \neq \ell} \tilde{u}_j^2 \right) \tilde{u}_\ell, \quad \ell \in [k].$$

Algorithm 1: A diffusion generated algorithm for computing Dirichlet partitions.

Input: Let U be a d -dimensional Euclidean subset or a closed surface,

$\tau > 0$ be a time-parameter, and $\mathbf{u}^0 \in H^1(U; \mathbb{R}^k)$ be an initial condition.

Output: An approximate ground state, $\mathbf{u}^s \in H^1(U; \mathbb{R}^k)$, satisfying (3).

for $s = 1, 2, \dots$ **do**

1. Diffusion Step. Solve the initial value problem for the diffusion equation until time τ with initial value given by each of the components of $\mathbf{u}^{s-1}(x)$:

$$\begin{aligned}\partial_t u_\ell(t, x) &= \Delta u_\ell(t, x) \\ A(0, x) &= u_\ell^{s-1}(x).\end{aligned}$$

Let $\tilde{u}_\ell(x) = u_\ell(\tau, x)$.

2. Projection Step. Set

$$u_\ell^*(x) = \begin{cases} \tilde{u}_\ell(x) & \text{if } \tilde{u}_\ell(x) = \max_{j \in [k]} \tilde{u}_j(x) \\ 0 & \text{otherwise} \end{cases}.$$

3. Renormalization Step. Set $u_\ell^s(x) = \frac{u_\ell^*(x)}{\|u_\ell^*(x)\|}$ where $\|\cdot\|$ denotes the $L^2(U)$ norm.

if (4) *is satisfied, then*

 STOP

This is precisely the gradient flow of the second term of the relaxed energy \mathbf{E}^ε . Numerically, this system is solved using the Gauss-Seidel method. However, the small parameter ε here restricts the mesh size and fats the interface between any two partitions. Also, the authors only considered 2-dimensional case there.

Another approach, developed in first [4], is based on a Schrödinger operator relaxation of (1) and was further used in [12, 13, 23, 24].

Other related ideas based on a stochastic interpretation can be found in [10, 11].

3. Implementation of Algorithm 1

In this section, we describe a numerical implementation of Algorithm 1 for d -dimensional flat tori and spheres. Although Algorithm 1 could in principle be implemented in more generality, our implementation relies on the Fast Fourier Transform (FFT) or Spherical Harmonic Transform (SHT).

3.1. Implementation for flat tori

In this section, we consider the implementation of Algorithm 1 on the computational domain $\Omega = [-1, 1]^d$ ($d = 2, 3, 4$) with edges identified (periodic boundary conditions).

The diffusion step in Algorithm 1 for partition ℓ is to solve

$$\partial_t u_\ell(t, x) = \Delta u_\ell(t, x) \quad x \in \Omega, t \geq 0, \quad (6a)$$

$$u_\ell(0, x) = u_\ell^{s-1}(x) \quad x \in \Omega \quad (6b)$$

$$u_\ell \text{ satisfies periodic boundary conditions on } \partial\Omega. \quad (6c)$$

It is well-known that the solution for the diffusion equation for a scalar function on \mathbb{R}^d at time $t = \tau$ can be expressed as the convolution of the heat kernel,

$$G_\tau^d(x) = (4\pi\tau)^{-\frac{d}{2}} \exp\left(-\frac{|x|^2}{4\tau}\right),$$

and the initial condition, $u_\ell^{s-1}(x)$. For our periodic domain, $\Omega \subset \mathbb{R}^d$, we denote by $G_{p,\tau}$ the periodic heat kernel, given by

$$G_{p,\tau}(x) = \sum_{\alpha \in \mathbb{Z}^d} G_\tau^d(x - \alpha).$$

The solution, $\tilde{u}_\ell(x) = u_\ell(\tau, x)$ to (6) at time $t = \tau$ has matrix components given by $\tilde{u}_\ell = G_{p,\tau} * u_\ell^{s-1}$, where $*$ denotes the convolution.

We denote the Fourier transform and its inverse by \mathcal{F} and \mathcal{F}^{-1} , respectively. Using the convolution property that $\mathcal{F}(G_{p,\tau} * u_\ell^{s-1}) = \mathcal{F}(G_{p,\tau}) \mathcal{F}(u_\ell^{s-1})$, we can express the solution to (6) as

$$\tilde{u}_\ell = \mathcal{F}^{-1} (\mathcal{F}(G_{p,\tau}) \mathcal{F}(u_\ell^{s-1})) .$$

In our numerical implementation, due to the periodic boundary condition, can efficiently compute an approximation to the Fourier transform and its inverse using the fast Fourier transform (FFT) and inverse fast Fourier transform (iFFT). That is, an approximate solution to (6) is evaluated via

$$\tilde{u}_\ell = \text{iFFT} (\text{FFT}(G_{p,\tau}) \text{FFT}(u_\ell^{s-1})) .$$

It is well known that the computational complexity of the FFT is $O(n^d \log n)$ where n is the number of grid points in each direction. The total computational complexity of this Algorithm 1 is then

$$(\#\text{steps}) \cdot k \cdot O(n^d \log n) .$$

3.2. Implementation on a spherical surface

In this section, we consider the implementation on the computational domain $\Omega = S^2$ which is a spherical surface with radius 1. Here is is understood that Δ is the Laplace-Beltrami operator on the spherical surface. We parameterize S^2 in spherical coordinates,

$$(x, y, z) = (\sin \theta \sin \phi, \sin \theta \cos \phi, \cos \theta), \quad (7)$$

where $\theta \in [0, \pi]$ is the inclination and $\phi \in [0, 2\pi]$ is the azimuth. It is well known that the eigenfunctions of the Laplace Beltrami operator on the spherical surface are the spherical harmonic functions, Y_l^m , where

$$Y_l^m(\theta, \phi) = \sqrt{\frac{(2l+1)}{4\pi} \frac{(l-m)!}{(l+m)!}} P_l^m(\cos(\theta)) e^{im\phi}, \quad l \in \mathbb{N}, \quad m \in \{-l, \dots, l\} .$$

with the corresponding eigenvalues being $-l(l+1)$. Denote SHT as the spherical harmonic transform and $iSHT$ as the inverse spherical harmonic transform. For

each partition ℓ , the initial condition $u_\ell(t = 0, x)$ can be decomposed by n^2 spherical harmonic functions:

$$u_\ell(t = 0, x) = \sum_{l=0}^n \sum_{m=-l}^l s_{l,m}^\ell Y_l^m.$$

Using the spherical harmonic functions to express the solution of the surface diffusion equation at $t = \tau$, the coefficients are given by $s_{l,m}^\ell e^{-l(l+1)\tau}$. The solution to the diffusion equation can be computed by the inverse spherical harmonic transform,

$$u_\ell(\tau, x) = iSHT \left(SHT(u_\ell(0, x)) e^{-l(l+1)\tau} \right).$$

4. Numerical results

In this section, we use the implementation of Algorithm 1, described in Section 2, to compute approximate Dirichlet partitions. The algorithms are implemented in MATLAB. For the results in two, three, and four dimensional periodic space, we used fast Fourier transform (FFT) to solve the heat diffusion equation; see in Sections 4.1, 4.2, and 4.3. For the results on the sphere, we used the spherical harmonic transform to solve the surface diffusion equation on a spherical surface; see Section 4.4. For all numerical results, we initialize the algorithm by computing the Voronoi tessellation for a random point set in U and use the normalized indicator functions for this tessellation. Below, we simply refer to this as *initializing using a random tessellation*. All reported results were obtained on a laptop with a 2.7GHz Intel Core i5 processor and 8GB of RAM.

To compare the energies between configurations and for different size domains and values of k , we consider the normalized energy

$$E(k, U) := \min_{U = \cup_\ell U_\ell} \frac{|U|^{\frac{2}{d}}}{k^{1+\frac{2}{d}}} \sum_{\ell=1}^k \lambda(U_\ell). \quad (8)$$

This quantity is invariant under homothety, *i.e.*, $E(k, \alpha U) = E(k, U)$ and has

the property that for $m \in \mathbb{N}$,

$$E(m^d k, mU) = \min_{\bigcup_{\ell} U_{\ell}} \frac{m^2 |U|^{\frac{2}{d}}}{m^{d+2} k^{1+\frac{2}{d}}} \sum_{\ell=1}^{m^d k} \lambda(U_{\ell}) = \min_{\bigcup_{\ell} U_{\ell}} \frac{|U|^{\frac{2}{d}}}{k^{1+\frac{2}{d}}} \frac{1}{m^d} \sum_{\ell=1}^{m^d k} \lambda(U_{\ell}) \leq E(k, U).$$

where the last inequality comes from repeating the k -Dirichlet partition on U — m times in each direction—to form a $m^d k$ -Dirichlet partition on mU . We report values for an approximation of E in (8), given by

$$\begin{aligned} \tilde{E}(k, U) &:= \frac{|U|^{\frac{2}{d}}}{k^{1+\frac{2}{d}}} \frac{1}{\tau} \left(k - \sum_{\ell=1}^k \langle u_{\ell}, e^{\Delta \tau} u_{\ell} \rangle \right) \\ &\approx \frac{|U|^{\frac{2}{d}}}{k^{1+\frac{2}{d}}} \sum_{\ell=1}^k \langle u_{\ell}, -\Delta u_{\ell} \rangle, \end{aligned} \quad (9)$$

where the $\{u_{\ell}\}_{\ell \in [k]}$ have unit $L^2(U)$ norm. See [19, 20] for more intuition on this approximate energy.

4.1. 2d flat torus

It was proven by T. Hales that the regular hexagon tessellation is the equal-area partition that minimizes surface area [25]. In two-dimensional Euclidean space, it has been conjectured that this tessellation is also a Dirichlet partition [2]. Computationally the problem of partitioning 2D rectangles, either with periodic or Dirichlet boundary conditions, has been addressed in [10, 21, 4, 12, 24] and embedded tori have been studied in [22, 24]. In all of these studies, for large values of k , regular hexagons are ubiquitous.

In Figure 1, we display Dirichlet partitions for the $[-1, 1]^2$ periodic domain discretized by 256^2 uniform grid points with $k = 3 - 9, 11, 12, 15, 16$ and 20. The code was executed several times initialized using random k -tessellations. For these values of k , the algorithm always converges to the same pattern, but for larger values of k , we observe local minima. In this experiment, we use $\tau = 0.0625$ for $k = 20$ and $\tau = 0.125$ for all other values of k . In Table 1, we display the average CPU time for each value of k . Here, the average CPU time is calculated by averaging the CPU time for each of the 10 experiments (with random initial conditions).

The partitions obtained are similar to those found previously. Since the domain has aspect ratio equal to one, regular hexagons cannot be used to tile the domain, so the hexagons are slightly distorted. To better see the irregular Dirichlet partitions for $k = 5$ and $k = 7$, in Figure 2, we plot their periodic extensions. These numerical results demonstrate that, although Algorithm 1 is simple, it is efficient and stable. In Table 1, we also tabulate the values of \tilde{E} in (9) for different values of k .

Table 1: Values of \tilde{E} in (9) and the average CPU time for different values of k .

k	3	4	5	6	7	8
\tilde{E}	2.39	2.13	2.23	2.18	2.17	2.09
Average CPU time (s)	3.02	1.89	5.09	3.49	6.89	6.36
k	9	11	12	15	16	20
\tilde{E}	2.11	2.09	2.03	1.97	1.99	1.70
Average CPU time (s)	9.89	11.02	8.42	16.18	21.45	35.38

4.2. 3d flat torus

In three dimensions, the minimal total surface area partition is unknown. Lord Kelvin conjectured that a packing of truncated octahedra was optimal [26]. However, R. Weaire and D. Phelan discovered another structure comprised of two polyhedra which has a slightly smaller surface area [27]. For the three-dimensional Dirichlet partitioning problem, as far as we are aware, very little is known analytically and only a few papers have investigated the problem computationally [11, 24]. Interestingly, both the Kelvin and the Weaire-Phelan structures appear as Dirichlet partitions, depending on the domain and value k . In this section, we compute Dirichlet partitions using Algorithm 1 for the periodic cube, $[-1, 1]^3$ and $k = 2, 4, 8, 16$.

For $k = 2$ and for every initialization using a random tessellation we tried, we obtained a partition given by a slab, which is shown in the left panel of Figure 3. If we choose an initial condition so that the interface is the implicit equation of

the surface, $\cos(x) + \cos(y) + \cos(z) = 0$, we obtain a partition that has interface that is similar to the Schwarz P surface, displayed in the right panel of Figure 3. These partitions are similar to ones reported in [11, 13]. In this experiment, the cube is discretized by 128^3 uniform grid points and $\tau = 0.25$. The CPU time for the first one is 26 seconds and the CPU time for the second one is 3 seconds.

For $k = 4$ and initialization using a random tessellation, we obtain a partition of the cube by four identical rhombic dodecahedron structures which is displayed in Figure 4. In this experiment, the cube is discretized by 128^3 uniform grid points and $\tau = 0.125$. The CPU time for this experiment is 112 seconds.

For $k = 8$ and initialization using a random tessellation, we obtain a partition of the cube that is similar to the Weaire-Phelan structure. Figure 5 displays different views of a periodic extension of the partition. Figures 6 and 7 display different views of the first and second type Weaire-Phelan structures. In this experiment, the cube is discretized by 128^3 uniform grid points and $\tau = 0.0625$. The CPU time for this experiment is 1200 seconds. A rougher, but similar result can also be obtained by discretizing the cube with 64^3 uniform grid points and using $\tau = 0.0625$ in 81 seconds. In the numerical experiments, our algorithm occasionally converged to other local minimizers. However, our experiments indicate that the algorithm usually converges to the Weaire-Phelan structure, implying that the basin of attraction for this structure is larger.

For $k = 16$ and initialization using a random tessellation, we obtain a partition of the cube that is a packing of truncated octahedra, similar to the structure Lord Kelvin studied. Figure 8 displays different views of a periodic extension of this partition. In this experiment, the cube is discretized by 128^3 uniform grid points and $\tau = 0.0625$. The CPU time for this experiment is 3556 seconds.

In Table 2, we also tabulate the values of \tilde{E} in (9), the CPU time, and the τ used for different values of k .

4.3. 4d flat torus

To our knowledge, neither partitions that minimize the total surface area or Dirichlet partitions in four dimensional space have been studied. In this

Table 2: Values of \tilde{E} in (9), the CPU time, and the τ used for different values of k .

k	2(left)	2(right)	4	8	16
\tilde{E}	3.43	3.61	3.07	2.68	2.47
CPU time (s)	26	3	112	1200	3556
τ	0.25	0.25	0.125	0.0625	0.0625

section, we compute Dirichlet partitions using Algorithm 1 for the tesseract, $[-1, 1]^4$, with periodic boundary conditions and $k = 4, 8$.

For $k = 4$ and initialization using a random tessellation, we obtain a constant extension of a rhombic dodecahedral honeycomb along the fourth direction. A rhombic dodecahedral honeycomb is plotted in Figure 4; we do not include a figure of this extension.

For $k = 8$ and initialization using a random tessellation, we obtain a partition of the tesseract as shown in Figure 9. The four columns of this plot correspond to slices perpendicular to the x_1 –, x_2 –, x_3 –, and x_4 –axes, respectively. The eight rows correspond to the slices at $x_j = -1, -0.75, -0.5, -0.25, 0, 0.25, 0.5$, and 0.75 , respectively. The partition obtained is known as a *24-cell honeycomb*, which is a tessellation by 24-cells. In the experiment, the tesseract was discretized by 64^4 grid points and $\tau = 0.0625$. The CPU time was 9803 seconds.

4.4. Results for Sphere

Finally, we consider Dirichlet partitions for a sphere. It has been conjectured that the 3 Dirichlet partition of the sphere is the “Y-partition” [28]. Dirichlet partitions have been computed on the sphere for several values of k , see [12, 22, 24]. In this section, we compute Dirichlet partitions using Algorithm 1 for the sphere. Our results are consistent with previous results.

In Figures 10 and 11, we display Dirichlet partitions on the sphere for $k = 3$ –7, 9, 10, 12, 14, and 20, obtained from an initialization using a random tessellation. In Table 3, the CPU times for each case are given. For parameterization as in (7), the inclination and azimuthal coordinates are discretized by 256^2 uniform

grid points and $\tau = 0.008$. Values of \tilde{E} in (9) for different values of k are displayed in Table 3.

Table 3: Values of \tilde{E} in (9) and the average CPU time for different values of k .

k	3	4	5	6	7
\tilde{E}	13.49	13.64	14.16	13.73	13.96
CPU time (s)	180	485	727	901	1231
k	9	10	12	14	20
\tilde{E}	13.65	13.54	13.08	12.95	12.20
CPU time (s)	2040	2165	1631	1769	9011

References

- [1] D. Bucur, G. Buttazzo, A. Henrot, Existence results for some optimal partition problems, *Adv. Math. Sci. Appl.* 8 (1998) 571–579.
- [2] L. A. Caffarelli, F. H. Lin, An Optimal Partition Problem for Eigenvalues, *J. Sci. Comp.* 31 (1-2) (2007) 5–18. [doi:10.1007/s10915-006-9114-8](https://doi.org/10.1007/s10915-006-9114-8).
- [3] B. Helffer, On Spectral Minimal Partitions: A Survey, *Milan J. Math.* 78 (2010) 575–590. [doi:10.1007/s00032-010-0129-0](https://doi.org/10.1007/s00032-010-0129-0).
- [4] B. Bourdin, D. Bucur, E. Oudet, Optimal Partitions for Eigenvalues, *SIAM Journal on Scientific Computing* 31 (6) (2010) 4100–4114. [doi:10.1137/090747087](https://doi.org/10.1137/090747087).
- [5] W. Bao, Ground states and dynamics of multicomponent Bose–Einstein condensates, *Multiscale Modeling & Simulation* 2 (2) (2004) 210–236. [doi:10.1137/030600209](https://doi.org/10.1137/030600209).
- [6] W. Bao, Q. Du, Computing the ground state solution of Bose–Einstein condensates by a normalized gradient flow, *SIAM Journal on Scientific Computing* 25 (5) (2004) 1674–1697. [doi:10.1137/s1064827503422956](https://doi.org/10.1137/s1064827503422956).
- [7] S.-M. Chang, C.-S. Lin, T.-C. Lin, W.-W. Lin, Segregated nodal domains of two-dimensional multispecies Bose–Einstein condensates, *Physica D: Nonlinear Phenomena* 196 (3) (2004) 341–361. [doi:10.1016/j.physd.2004.06.002](https://doi.org/10.1016/j.physd.2004.06.002).

- [8] M. Conti, S. Terracini, G. Verzini, Nehari's problem and competing species systems, *Annales de l'IHP Analyse Nonlinéaire* 19 (6) (2002) 871–888. [doi:10.1016/s0294-1449\(02\)00104-x](https://doi.org/10.1016/s0294-1449(02)00104-x).
- [9] M. Conti, S. Terracini, G. Verzini, An optimal partition problem related to nonlinear eigenvalues, *Journal of Functional Analysis* 198 (1) (2003) 160–196. [doi:10.1016/s0022-1236\(02\)00105-2](https://doi.org/10.1016/s0022-1236(02)00105-2).
- [10] O. Cybulska, V. Babin, R. Holyst, Minimization of the Renyi entropy production in the space-partitioning process, *Physical Review E* 71 (4) (2005) 46130. [doi:10.1103/physreve.71.046130](https://doi.org/10.1103/physreve.71.046130).
- [11] O. Cybulska, R. Holyst, Three-dimensional space partition based on the first Laplacian eigenvalues in cells, *Physical Review E* 77 (5) (2008) 56101. [doi:10.1103/physreve.77.056101](https://doi.org/10.1103/physreve.77.056101).
- [12] B. Osting, C. D. White, E. Oudet, Minimal Dirichlet energy partitions for graphs, *SIAM J. Scientific Computing* 36 (4) (2014) A1635–A1651. [doi:10.1137/130934568](https://doi.org/10.1137/130934568).
- [13] D. Zosso, B. Osting, A minimal surface criterion for graph partitioning, *AIMS Inverse Problems and Imaging* 10 (4) (2016) 1149–1180. [doi:10.3934/ipi.2016036](https://doi.org/10.3934/ipi.2016036).
- [14] B. Osting, T. H. Reeb, Consistency of dirichlet partitions, *SIAM Journal on Mathematical Analysis* 49 (5) (2017) 4251–4274. [doi:10.1137/16m1098309](https://doi.org/10.1137/16m1098309).
- [15] B. Merriman, J. K. Bence, S. Osher, Diffusion generated motion by mean curvature, *UCLA CAM Report* 92-18, 1992.
- [16] B. Merriman, J. K. Bence, S. J. Osher, Motion of multiple junctions: A level set approach, *J. Comput. Phys.* 112 (2) (1994) 334–363. [doi:10.1006/jcph.1994.1105](https://doi.org/10.1006/jcph.1994.1105).
- [17] B. Merriman, J. Bence, S. Osher, Diffusion generated motion by mean curvature, *AMS Selected Letters, Crystal Grower's Workshop* (1993) 73–83.
- [18] S. J. Ruuth, B. Merriman, J. Xin, S. Osher, Diffusion-generated motion by mean curvature for filaments, *Journal of Nonlinear Science* 11 (6) (2001) 473–493. [doi:10.1007/s00332-001-0404-x](https://doi.org/10.1007/s00332-001-0404-x).

- [19] S. Esedoglu, F. Otto, Threshold dynamics for networks with arbitrary surface tensions, *Communications on Pure and Applied Mathematics* 68 (5) (2015) 808–864. [doi:10.1002/cpa.21527](https://doi.org/10.1002/cpa.21527).
- [20] B. Osting, D. Wang, A generalized MBO diffusion generated motion for orthogonal matrix-valued fields, *arXiv preprint, arXiv:1711.01365* (2017).
- [21] Q. Du, F. Lin, Numerical approximations of a norm-preserving gradient flow and applications to an optimal partition problem, *Nonlinearity* 22 (1) (2008) 67–83. [doi:10.1088/0951-7715/22/1/005](https://doi.org/10.1088/0951-7715/22/1/005).
- [22] C. M. Elliott, T. Ranner, A computational approach to an optimal partition problem on surfaces, *Interfaces and Free Boundaries* 17 (2015) 353–379. [doi:10.4171/IFB/346](https://doi.org/10.4171/IFB/346).
- [23] B. Bogosel, B. Velichkov, A multiphase shape optimization problem for eigenvalues: Qualitative study and numerical results, *SIAM Journal on Numerical Analysis* 54 (1) (2016) 210–241. [doi:10.1137/140976406](https://doi.org/10.1137/140976406).
- [24] B. Bogosel, Efficient algorithm for large spectral partitions, *arXiv preprint arXiv: 1705.08739*.
- [25] T. C. Hales, The honeycomb conjecture, *Discrete & Computational Geometry* 25 (1) (2001) 1–22. [doi:10.1007/s004540010071](https://doi.org/10.1007/s004540010071).
- [26] W. Thompson, On the division of space with minimum partitional area, *Acta Mathematica* 11 (1-4) (1887) 121–134. [doi:10.1007/BF02612322](https://doi.org/10.1007/BF02612322).
- [27] D. Weaire, R. Phelan, A counter-example to Kelvin’s conjecture on minimal surfaces, *Philosophical Magazine Letters* 69 (2) (1994) 107–110. [doi:10.1080/09500839408241577](https://doi.org/10.1080/09500839408241577).
- [28] B. Helffer, T. Hoffmann-Ostenhof, S. Terracini, On spectral minimal partitions: the case of the sphere, in: *Around the Research of Vladimir Maz’ya III*, Springer, 2010, pp. 153–178.

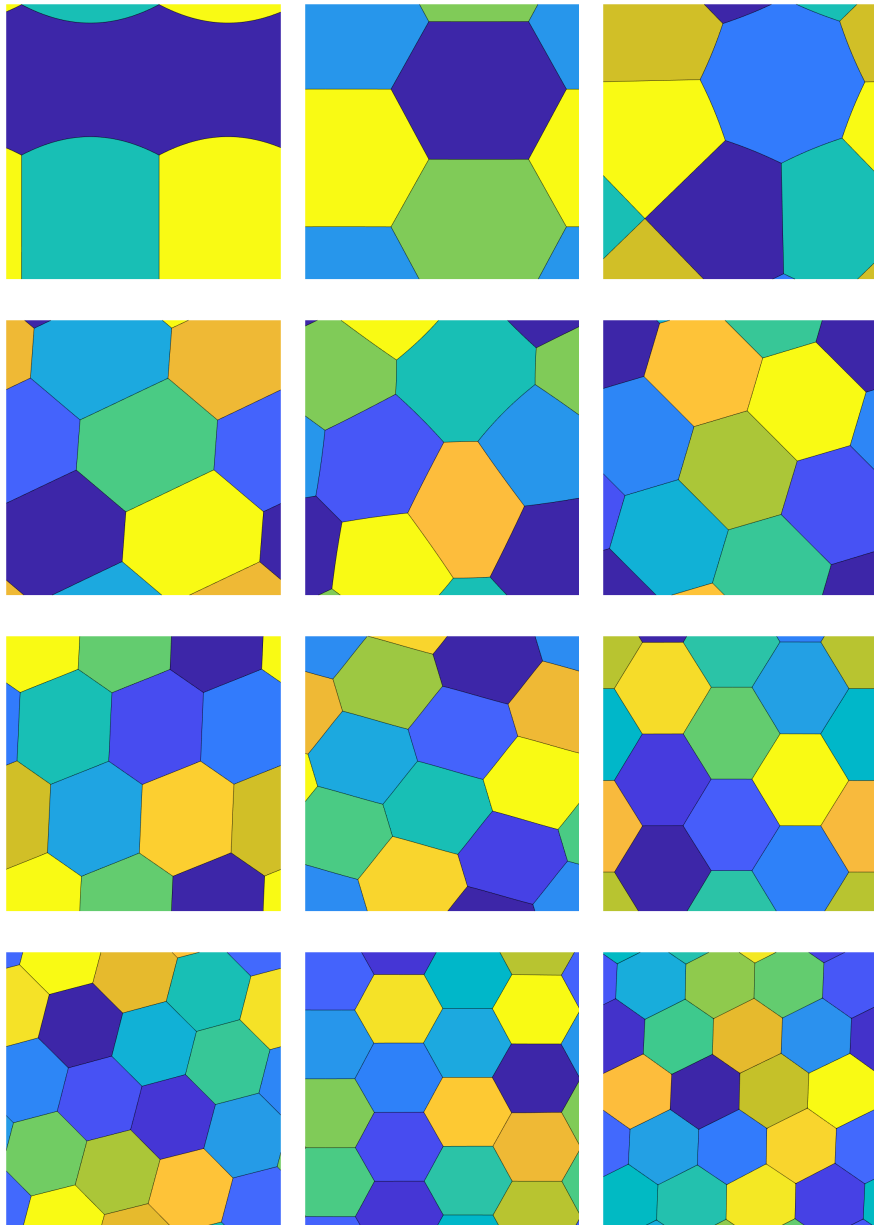


Figure 1: From left to right and top to bottom: Dirichlet partitions on the $[-1, 1]^2$ periodic domain discretized by 256^2 uniform grid points with $k = 3, 9, 11, 12, 15, 16$, and 20. The last one is computed using $\tau = 0.0625$ while others are all computed using $\tau = 0.125$. The average CPU time for each case is 3.02, 1.89, 5.09, 3.49, 6.89, 6.36, 9.89, 11.02, 8.42, 16.18, 21.45, and 35.38 seconds respectively.

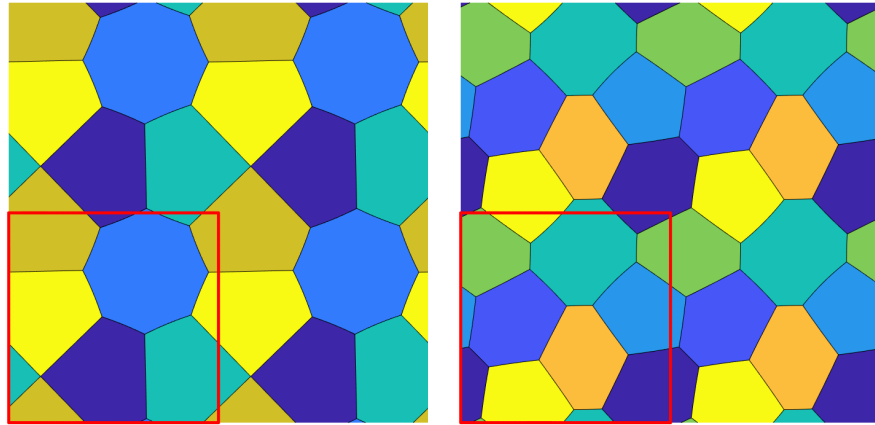


Figure 2: The periodic extension of the $k = 5$ (left) and $k = 7$ (right) Dirichlet partitions to a larger domain. In both panels, the red lines are the boundary of $[-1, 1]^2$. See Figure 1.

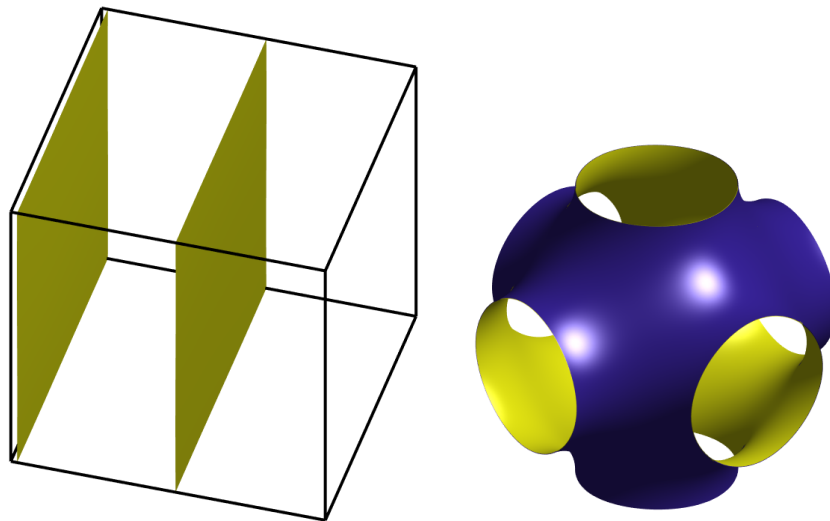


Figure 3: **(left)** A $k = 2$ Dirichlet partition of the periodic cube $[-1, 1]^3$ with interface given by parallel planes. **(right)** The periodic cube $[-1, 1]^3$ is partitioned into two components by a surface that is similar to the Schwarz P surface. In this experiment, the cube is discretized by 128^3 uniform grid points and $\tau = 0.25$. The CPU time for the left case is 26 seconds while the CPU time for the right case is 3 seconds.

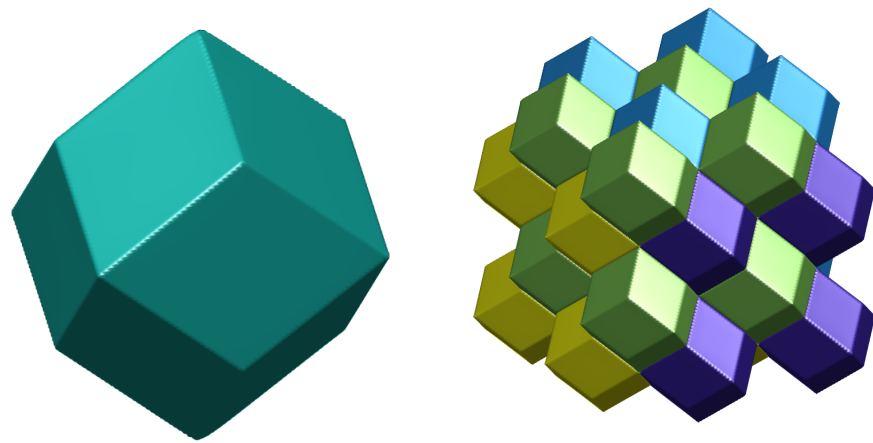


Figure 4: A $k = 4$ Dirichlet partition of the periodic cube, $[-1, 1]^3$ consisting of rhombic dodecahedra (left). On the right, we periodically extend the obtained partition to show how the rhombic dodecahedra fit together. In this experiment, the cube is discretized by 128^3 grid points and $\tau = 0.125$. The CPU time for this experiment is 112 seconds.

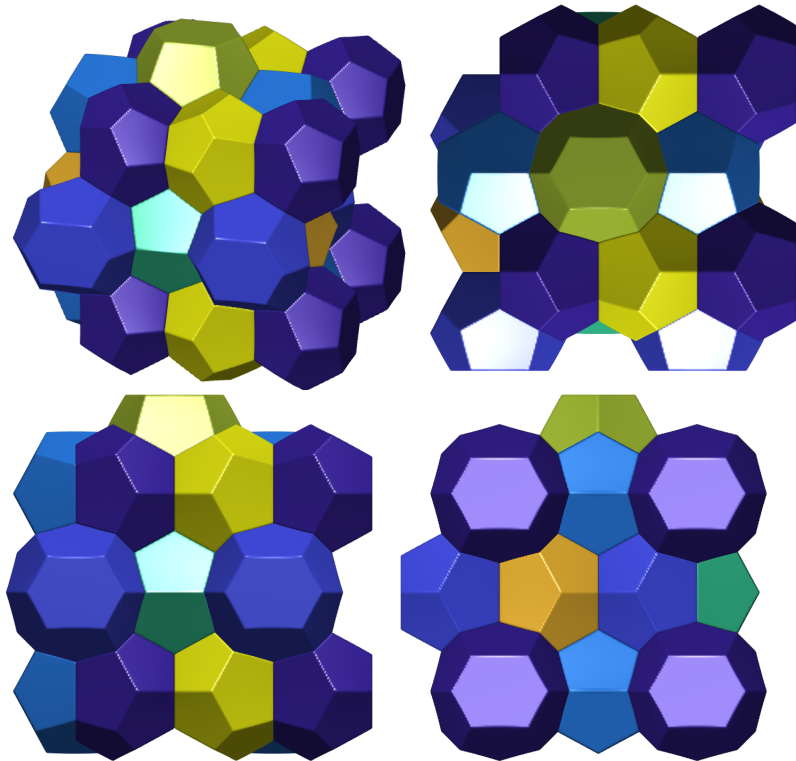


Figure 5: A $k = 8$ Dirichlet partition of the periodic cube, $[-1, 1]^3$, which is similar to the Weaire-Phelan structure. The different panels show a 3d view (top left), a vertical view (top right), a front view (bottom left), and a side view (bottom right). There are 6 type-one Weaire-Phelan structures and 2 type-two Weaire-Phelan structures in the partition; see Figures 6 and 7 for plots of these structures. In each panel, we have extended the partition periodically, so that it is easier to see how the structures fit together. In this experiment, the cube is discretized by 128^3 uniform grid points and $\tau = 0.0625$. The CPU time for this experiment is 1200 seconds.

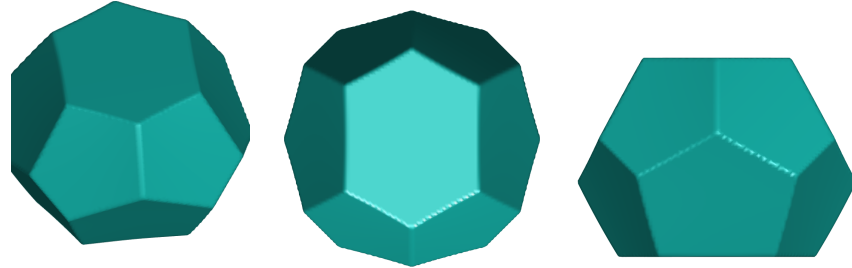


Figure 6: **(left)** A type-one Weaire-Phelan structure, **(center)** a vertical view, and **(right)** a front view. The side view is same as the front view.

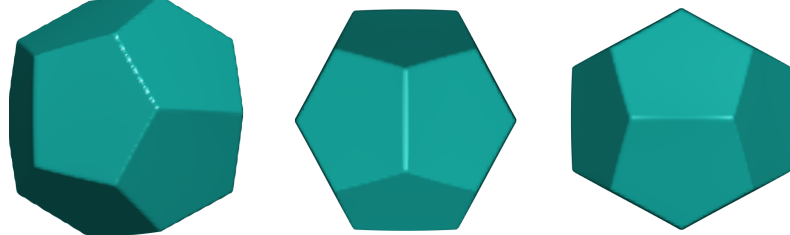


Figure 7: **(left)** A type-two Weaire-Phelan structure, **(center)** a vertical view, and **(right)** a front view. The side view is same as the vertical view.

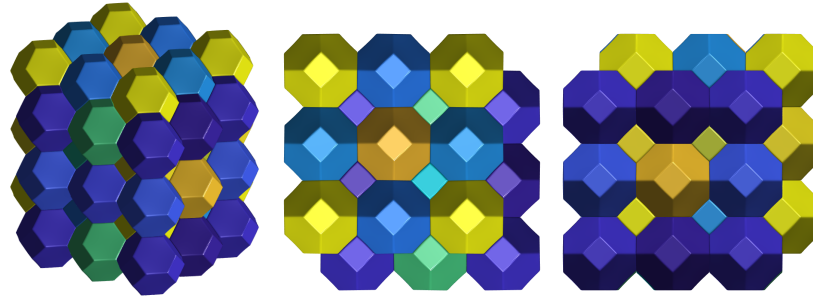


Figure 8: **(left)** A $k = 12$ Dirichlet partition of the periodic cube, $[-1, 1]^3$, by equal truncated octahedra, similar to Kelvin's structure. The partition has been periodically extended. **(center)** A vertical view. **(right)** A side view. The front view is same as the vertical view. In this experiment, the cube is discretized by 128^3 uniform grid points and $\tau = 0.0625$. The CPU time for this experiment is 3556 seconds.

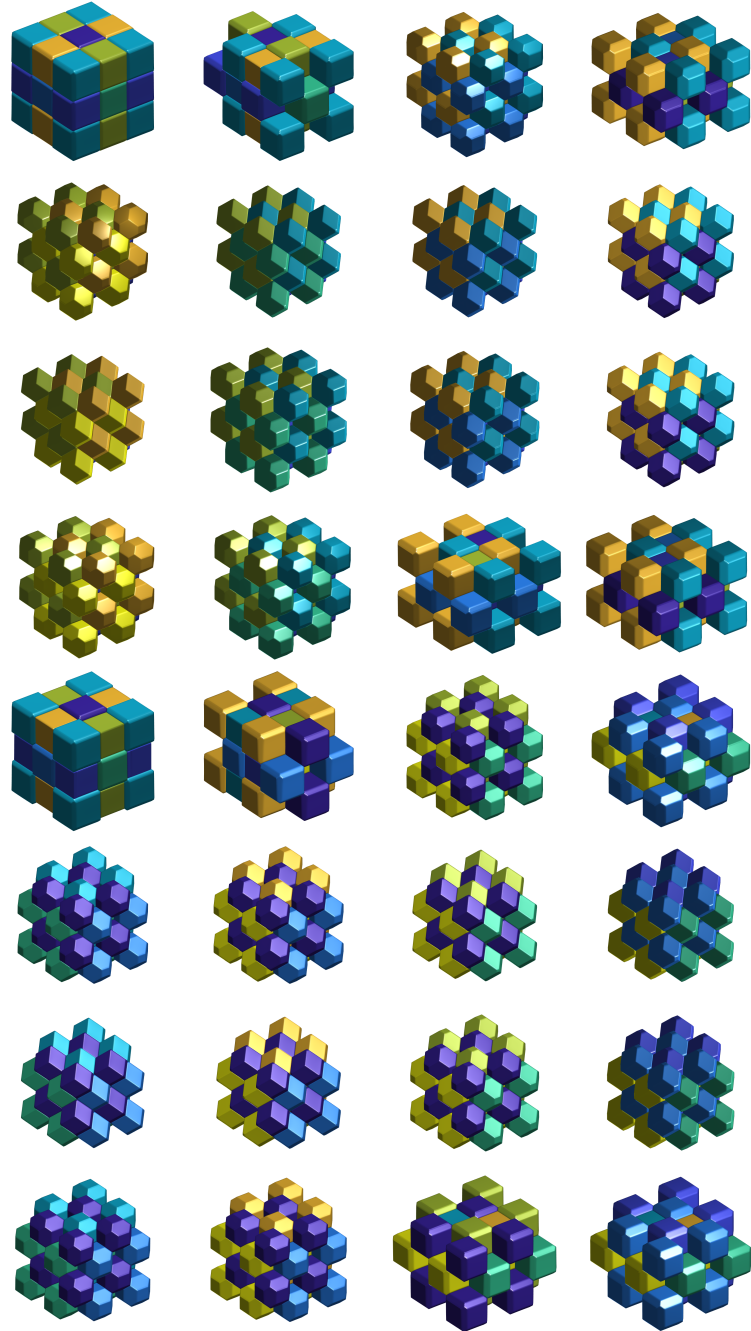


Figure 9: A $k = 8$ Dirichlet partition of the periodic tesseract, $[-1, 1]^4$, by 24-cells. The four columns correspond to the slides perpendicular to the x_1 -, x_2 -, x_3 -, and x_4 -axis respectively. The eight rows correspond to the slices at $x_j = -1, -0.75, -0.5, -0.25, 0, 0.25, 0.5, 0.75$, respectively. The CPU time was 9803 seconds.

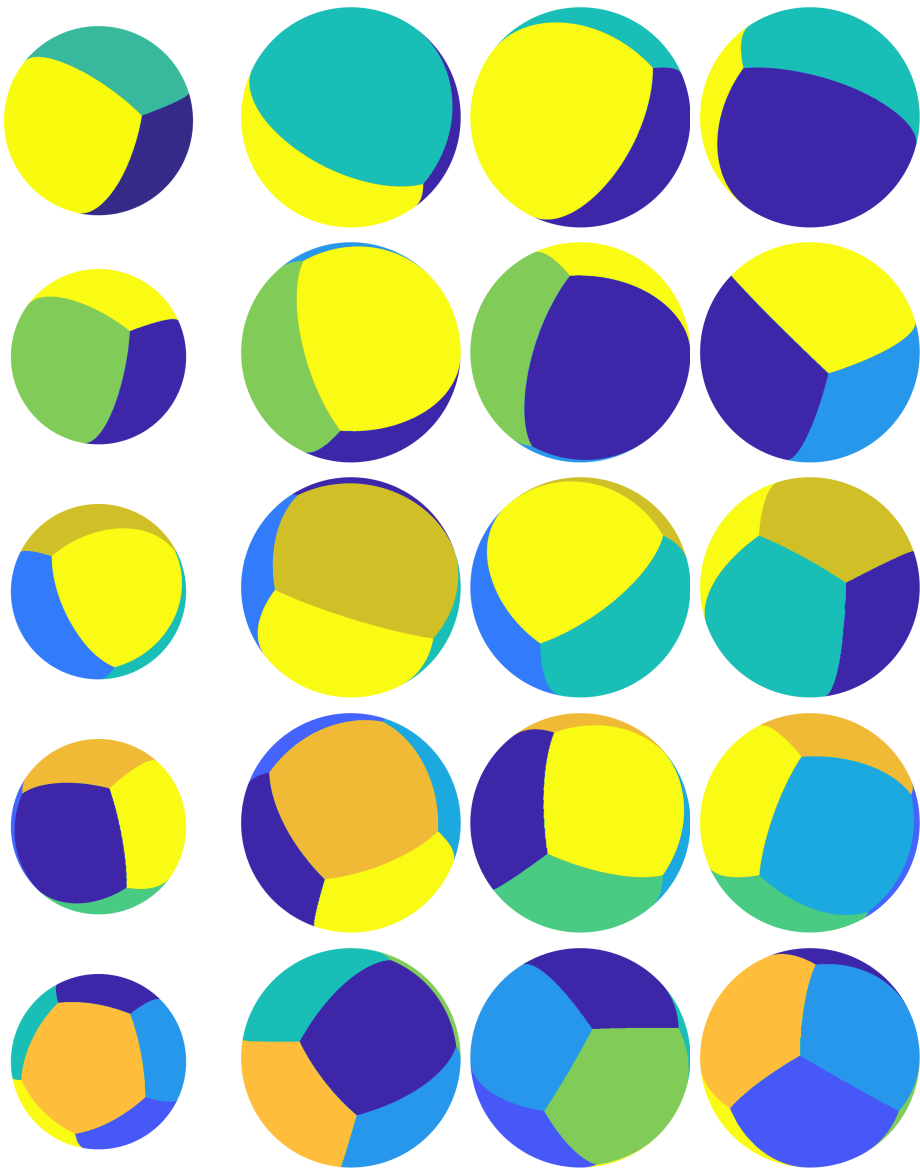


Figure 10: Column 1: k -Dirichlet partitions of a sphere. Column 2: Vertical view. Column 3: Front view. Column 4: Side view. From top to bottom: k -Dirichlet partitions of a sphere with $k = 3\text{--}7$. The CPU time for each case was 180, 485, 727, 901, and 1231 seconds respectively.

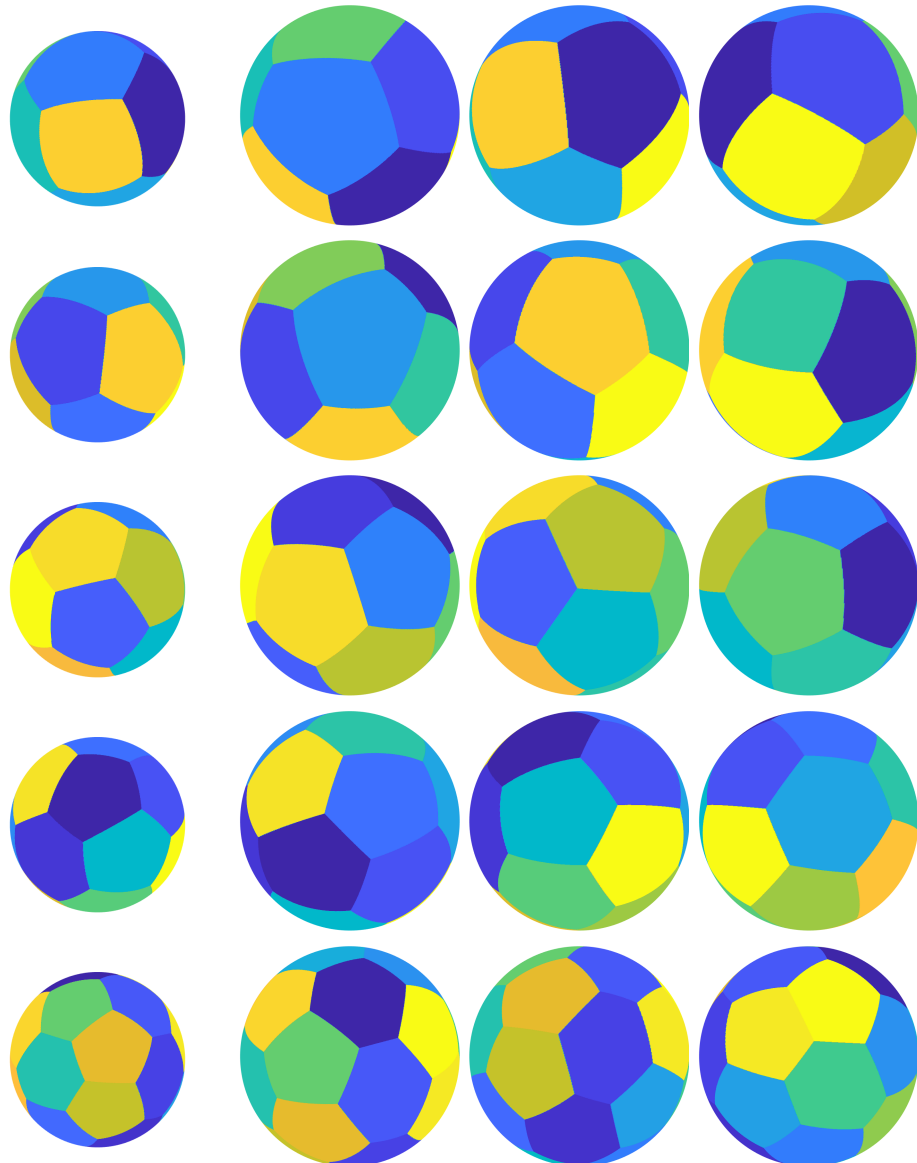


Figure 11: Column 1: k -Dirichlet partitions of a sphere. Column 2: Vertical view. Column 3: Front view. Column 4: Side view. From top to bottom: k -Dirichlet partitions of a sphere with $k = 9, 10, 12, 14$, and 20 . The CPU time for each case was 2040, 2165, 1631, 1769, and 9011 seconds respectively.